

Susceptibility Assessment of Shallow Landslides in Hulu Kelang Area, Kuala Lumpur, Malaysia Using Analytical Hierarchy Process and Frequency Ratio

Nader Saadatkhah · Azman Kassim ·
Lee Min Lee

Received: 7 October 2013 / Accepted: 8 September 2014 / Published online: 11 November 2014
© Springer International Publishing Switzerland 2014

Abstract Hulu Kelang is known as one of the most landslide susceptible areas in Malaysia. From 1990 to 2011, a total of 28 landslide events had been reported in this area. This paper compares two models as Analytical Hierarchy Process (AHP) and probability–frequency ratio (FR) methods for recognizing landslide susceptibility regions in the Hulu Kelang area. Eleven landslide influencing factors were considered to form the probability–FR and AHP matrix, i.e. lithology–weathering, land cover, curvature, slope inclination, slope aspect, drainage density, elevation, distance to lake and stream, distance to road and trenches, the Stream Power Index and the Topographic Wetness Index. The accuracy of the maps produced from the two models were verified using a receiver operating characteristics. The verification results indicated that the probability–FR model based on probabilistic analysis of spatial distribution of historical landslide events was capable of producing a more reliable landslide susceptibility map in this study area compared to AHP model. About 89 % of the landslide

locations have been predicted accurately by using the FR map.

Keywords Landslide susceptibility · Landslide mapping · Probability–frequency ratio · Bivariate approach · Analytical hierarchy process

1 Introduction

Landslides are one of the most common geohazards in many parts of the world. The frequency of landslide occurrences increases with growing human population. The needs of protecting natural and agricultural areas have further pressed human developments ever closer to unstable slopes. To minimize losses incurred by landslides, it is essential to develop a good understanding of their causative factors which are useful for assessing landslide susceptibility of an area. The identification of landslide-prone regions is useful for carrying out quicker and safer mitigation programs, as well as future development planning of the area.

GIS based Criteria Decision Making (MCDM) has recently emerged as a multi criterion analysis method that enables incorporation of data retrieved from various sources for landslide assessment. MCDM implies a process of assigning values to alternatives that are evaluated along multi-criteria (Phua and Minowa 2005). One of the widely used GIS-MCDM techniques is known as analytical hierarchy process (AHP; Saaty 1980; Saaty and Vargas 2001). AHP

N. Saadatkhah (✉) · A. Kassim
Department of Geotechnics and Transportation, Faculty of
Civil Engineering, Universiti Teknologi Malaysia,
81300 Skudai, Malaysia
e-mail: snader4@live.utm.my

L. M. Lee
Faculty of Engineering and Science, Universiti Tunku
Abdul Rahman, 53300 Kuala Lumpur, Malaysia

method provides a flexible and easily understood way of analyzing complex technological problems. And other GIS-MCDM technique is frequency ratio (FR) model that use a numerical assessment of the relationship between slope instability and other controlling factors. Probability frequency ratio method focuses on historical correlations between landslide-controlling parameters and the distribution of landslide events.

The goal of this study was to compare and evaluate both AHP approaches and probabilistic frequency ratio model for their ability to assess the landslide susceptibility of a case study. The first step was to set parameter weights and combined the decision alternatives with AHP to create a landslide susceptibility map. The probabilistic frequency ratio draws on data regarding the distribution and effectiveness of factors that cause landslides to determine the correlation between regions and these factors (Lee 2005). Finally, the landslide susceptibility maps created as a result of this process are subjected to a comprehensive validation process. The models are validated using either data for landslides that was used to create the map or independent landslide information can be uses (Chung and Fabbri 2003; Guzzetti et al. 2006). This study used landslide data that was divided in two groups, a modeling group (70 % of the total landslide events) and a prediction group (30 % of the total landslide events). The modeling group was used as a training set for the development of landslide susceptibility maps that built on the two models discussed earlier (AHP, probabilistic frequency ratio models) while the prediction group was used for verification purposes.

2 Background of Study Area

Hulu Kelang is known as one of the most landslide prone areas in Malaysia. The area is located at the suburb of Kuala Lumpur, the capital city of Malaysia between 3°09'25" and 3°13'45"E longitude and 101°44'13" and 101°47'51"N latitude (Fig. 1). The average annual rainfall is about 2,440 mm in this area. The rainfall distributions are mainly characterized by two monsoon seasons, namely the Southwest monsoon from late May to September and the Northeast monsoon from November to March.

Soil investigations from previous studies revealed that the area is generally underlain by coarse-grained

granite (Ali 2000). Weathering of the granite produced sandy clay residual soil of approximately 15–30 m thick at the areas of high elevation. The residual soil layer becomes thinner on the mid-course of slopes, followed by exposed granite at the low elevation areas. Most of the slip planes of landslides developed within the residual soil layer. Somehow, the area has been constantly hit by fatal shallow landslides. From 1990 to 2011, a total of 28 major landslide incidents had been reported in this area.

3 Layers of Landslide Influencing Information

ArcGIS 10 with Spatial Analyst was used in the present study. To perform a reliable landslide susceptibility assessment, it is important to incorporate multiple layers of relevant information into the GIS system. Eleven layers of information, which can be broadly grouped into GIS as lithology-weathering, land cover, curvature, slope inclination, slope aspect, drainage density, elevation, distance to lake and stream, distance to road and trenches, the Stream Power Index (SPI) and the Topographic Wetness Index (TWI) were identified for processing relevant results. All the layers were digitalized into GIS format and their correlation, expressed in hazard index, with landslide occurrence was established using actual landslide data.

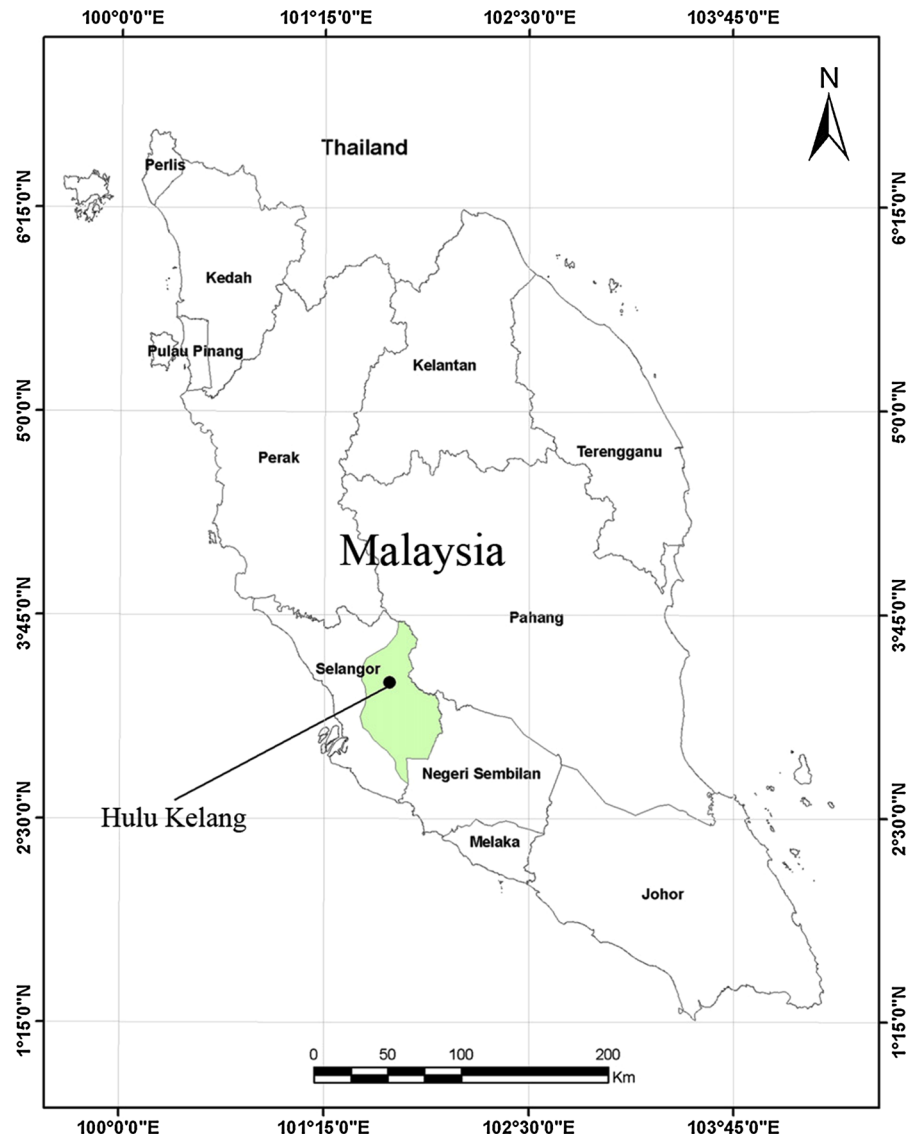
3.1 Landslide Inventory Map

Landslide inventory maps illustrate the distribution and locations of past landslides without indicating the mechanisms that triggered them. According to the data sources from the Ampang Jaya Municipal Council (MPAJ) and the Slope Engineering Branch of Public Works Department Malaysia (PWD), as well as data compilation from the previous reported studies by Farisham (2007), and Low and Ali (2012), a total of 28 major historical landslide events have been reported in the Hulu Kelang area from 1990 to 2011 (Fig. 2a).

3.2 Lithology-Weathering

The types of regolith material has a strong correlation with slope instability (Derbyshire et al. 2000;

Fig. 1 Location of Hulu Kelang area, Kuala Lumpur, Malaysia



D'Amato Avanzi et al. 2004; Wakatsuki et al. 2005; Sidle and Ochiai 2006). Weathering alters the mechanical, mineralogical and hydrologic attributes of regolith (Chigira 2002; Wakatsuki et al. 2005), and it is suggested that the effect is even more profound in tropical regions like Malaysia. Geological map at Hulu Kelang (Fig. 2b) revealed that the area is generally underlain by granitic rocks, phyllite-schist, and limestone with minor intercalations of phyllite. More than 90 % of the historical shallow landslides in Hulu Kelang occurred on highly/completely weathered granitic rock formation (Table 1).

3.3 Landcover

Landcover is an important extrinsic factor for slope stability. For instances, vegetated areas tend to reduce the action of climatic agents such as rainfall infiltration. Thus, a vegetated slope should possess lower landslide susceptibility than a barren slope. The landcover map in this study area was classified by the Department of Survey and Mapping Malaysia (JUPEM). Under the classification system, nine different types of landcovers were identified, i.e. primary forest, secondary jungle, rubber, resort and

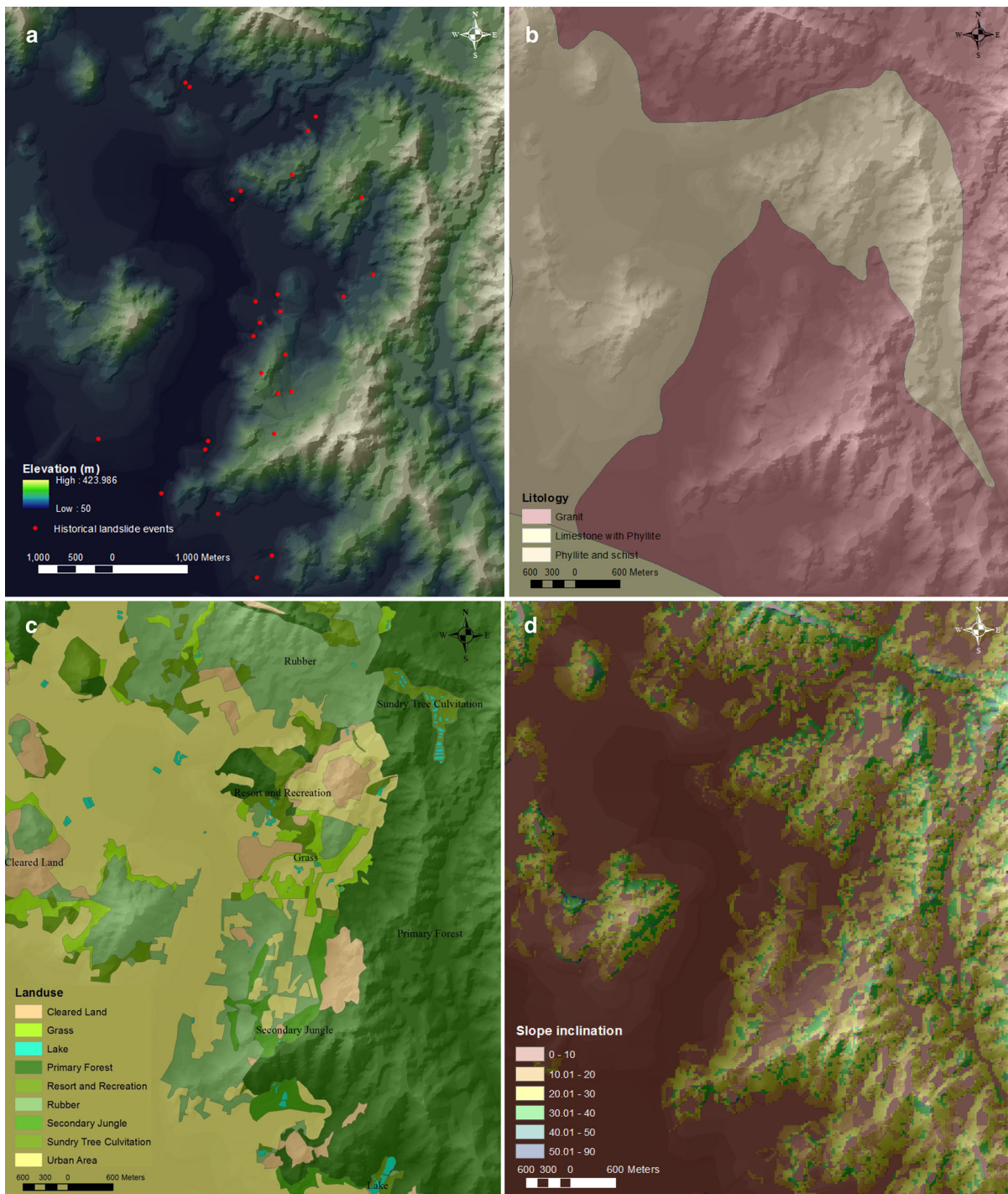


Fig. 2 a Landslide inventory map of Hulu Kelang area b Litology c Land cover d Slope inclination

recreation, sundry tree cultivation, grass, cleared land, urban area, and lake while, resort and recreation cover is in combination with urban area (Fig. 2c). Historical

slope failures were mainly scattered on the rubber plantation as a crop agriculture area and grassland areas in the Southeast Asia. These areas have

Table 1 AHP and frequency ratio values of the data layers

Factor	Class	% of total area	% of landslide area	AHP			Frequency ratio
				Third level (C)	Second level (B)	Final weights	
Lithology	Granite	54.08	44.08	0.571	0.216	0.123	1.345
	Physchist	42.51	16.53	0.286		0.062	0.642
	Limestone	3.41	0.00	0.143		0.031	0.000
Landcover	Prim. forest	31.61	7.35	0.04	0.154	0.006	0.383
	Sec. forest	1.88	2.20	0.158		0.024	1.934
	Rubber	14.29	21.67	0.285		0.044	2.502
	Sundry tree cultivation	1	0.00	0.04		0.006	0.000
	Grass	2.87	3.67	0.315		0.049	2.112
	Cleared land	4.64	2.57	0.082		0.013	0.914
	Urban area	43.25	23.14	0.04		0.006	0.883
Slope inclination	Lake	0.47	0.00	0.04		0.006	0.000
	0–10	56.69	32.32	0.035	0.154	0.005	0.941
	10–20	15.16	15.43	0.069		0.011	1.679
	20–30	22.01	9.92	0.148		0.023	0.743
	30–40	5.54	2.20	0.193		0.030	0.656
	40–50	0.49	0.73	0.259		0.040	2.474
	50–90	0.11	0.00	0.296		0.046	0.000
Slope aspect	North	5.77	6.61	0.024	0.118	0.003	1.891
	Northeast	5.08	2.57	0.113		0.013	0.835
	East	7.5	7.35	0.215		0.025	1.616
	Southeast	8.75	0.37	0.093		0.011	0.069
	South	8.08	7.71	0.024		0.003	1.575
	Southwest	8.75	3.67	0.134		0.016	0.693
	West	10.77	1.47	0.215		0.025	0.225
	Northwest	7.93	8.45	0.134		0.016	1.758
Plan curvature	Flat	37.37	22.41	0.049		0.006	0.989
	Concave	34.87	23.88	0.588	0.084	0.049	1.130
	Flat	30.89	17.63	0.089		0.007	0.942
Elevation	Convex	34.24	19.10	0.323		0.027	0.920
	0–100	48.24	34.89	0.467	0.046	0.021	1.194
	100–200	31.92	25.71	0.277		0.013	1.329
	200–300	17.99	0.00	0.16		0.007	0.000
	300–425	1.85	0.00	0.095		0.004	0.000
Distance to the roads and trenches	0–25	10.13	11.75	0.442	0.050	0.022	1.915
	25–50	13.22	19.83	0.228		0.011	2.476
	50–75	7.22	1.47	0.112		0.006	0.336
	75–100	5.82	2.94	0.091		0.005	0.833
	100–125	5.04	6.61	0.07		0.004	2.165
	125<	58.57	18.00	0.056		0.003	0.507

Table 1 continued

Factor	Class	% of total area	% of landslide area	AHP			Frequency ratio
				Third level (C)	Second level (B)	Final weights	
Distance to lake and streams	0–25	12.29	6.61	0.391	0.052	0.020	0.888
	25–50	22.11	9.92	0.175		0.009	0.740
	50–75	12.51	8.45	0.14		0.007	1.114
	75–100	8.74	3.31	0.078		0.004	0.624
	100–150	10.96	2.20	0.059		0.003	0.332
	150–200	5.86	2.57	0.059		0.003	0.724
	200–250	5.26	7.35	0.049		0.003	2.304
	250<	22.26	16.53	0.049		0.003	1.225
Drainage density	0–0.0025	44.22	11.75	0.102	0.056	0.006	0.439
	0.0025–0.005	8.69	0.00	0.046		0.003	0.000
	0.005–0.0075	8.88	2.94	0.09		0.005	0.546
	0.0075–0.01	14.17	19.10	0.127		0.007	2.224
	0.01–0.0125	10.89	15.06	0.235		0.013	2.282
	0.0125–0.015	9.74	11.75	0.296		0.017	1.991
	0.015–0.03	0.62	0.00	0.052		0.003	0.000
	0.03–0.135	2.78	0.00	0.052		0.003	0.000
Topographic wetness index (TWI)	6–9.32	0.00	0.00	0.081	0.039	0.003	0.858
	9.32–11.04	0.62	0.00	0.043		0.002	0.000
	11.04–12.76	7.58	4.85	0.043		0.002	0.000
	12.76–14.48	11.61	24.24	0.132		0.005	0.640
	14.48–16.2	3.09	6.06	0.409		0.016	2.089
	16.2–17.9	0.59	0.61	0.159		0.006	1.962
	17.9–19.3	0.59	0.00	0.043		0.002	1.025
Stream power index (SPI)	6–8.74	1.15	0.61	0.086	0.031	0.003	0.000
	8.74–10.44	0.94	0.00	0.086		0.003	0.858
	10.44–12.15	3.08	6.06	0.04		0.001	0.526
	12.15–13.85	11.88	13.94	0.362		0.011	0.000
	13.85–15.56	7.53	14.55	0.111		0.003	1.968
	15.56–16.6	0.51	0.00	0.275		0.009	1.173

undergone land cover change processes, i.e. progressive forest clearing, and conversion to rubber plantation or grassland (Table 1).

3.4 Slope Inclination

The factor of safety of a slope is defined by ratio of resistive force to sliding force. The sliding force is a function of slope angle. The steeper the slope, the larger the sliding force, and hence the lower the factor of safety of the slope (Saha et al. 2002; Cevik and Topal 2003; Ercanoglu et al. 2004; Lee et al. 2004a,b;

Lee 2005; Yalcin 2008). In the present study, the slope angles were divided into five categories, i.e. 0°–10°, 10°–20°, 20°–30°, 30°–50°, and >50° (Fig. 2d). Based on the distributions of the historical landslide events, it was found that 98.8 % of the landslides occurred on slopes between 0° and 40° (Table 1).

3.5 Slope Aspect

Aspect affects hydrologic processes of slopes via evapotranspiration. The hydrologic process, in turn, governs the weathering process, vegetation and root

development in soil slopes, particularly in dry environments (Sidle and Ochiai 2006). In this study, the aspect map was generated from DEM under nine categories, i.e. flat area (-1°), north ($337.5^\circ-22.5^\circ$), northeast ($22.5^\circ-67.5^\circ$), east ($67.5^\circ-112.5^\circ$), southeast ($112.5^\circ-157.5^\circ$), south ($157.5^\circ-202.5^\circ$), southwest ($202.5^\circ-247.5^\circ$), west ($247.5^\circ-292.5^\circ$), and northwest ($292.5^\circ-337.5^\circ$). Observations from the landslide inventory map revealed that about 48.5 % of the landslides occurred on the slopes inclined to NE, SW directions (Table 1).

3.6 Plan Curvature

Plan curvature generally refers to geometry of the earth surface and it describes how the inclination or aspect of a slope changes (Wilson and Gallant 2000; Nefeslioglu et al. 2008). In this study, three zones were identified based on their plan curvatures: positive curvature (convex), negative curvature (concave), and zero curvature representing flat surface. The analysis of landslide distribution density showed that 40 % of the landslides located in the concave zone, while 31 % of the landslides occurred in the convex zone (Table 1).

3.7 Elevation (DEM)

Figure 2a shows the digital elevation model (DEM) of the study area from the mean sea level (MSL). Elevation has an important influence on earth surface and topographic attributes. These attributes often account for spatial variability of different landscape processes such as vegetation distribution that are influenced by topographic effects. At this study, the DEM was derived using photogrammetric techniques. A series of aerial photographs from 1966 to 2003 were provided by department of surveying and mapping Malaysia (JUPEM). The cloud of photographic points extracted from aerial photographs data was therefore imported into a GIS environment. In addition to the points obtained using the photogrammetric analysis, the contour lines of the Regional Topographical Map at a 1:10,000 scale is extracted in standard topographic Ampang and Kampung Kelang Gates Baharu maps. In this study, five categories of elevations were identified, i.e. 0–50, 50–100, 100–200, 200–300, and >300 m. Most of the landslide distribution densities

occurred at 0–100 m (57.6 %) and 100–200 m (42.4 %) (Table 1).

3.8 Distance to the Roads and Trenches

Distance to roads and trenches could be a controlling factor for slope stability (Ayalew and Yamagishi 2005; Yalcin 2005). Road construction activities such as soil excavation, imposing of surcharge load, removal of vegetation cover may cause failures to the slopes which are otherwise stable. Six buffers were created based on the distance to roads, i.e. 0–25, 25–50, 50–75, 75–100, 100–125, and >125 m. About 86 % of past slides occurred 0–50 m from a roadway (Table 1).

3.9 Distance to Lake and Streams

It is essential to analyze the stream networks in landslide assessments because subsurface flows control the direction of groundwater movement, influence both the temporal and spatial pore-water pressure distribution in soil, and consequently alter the stability of slopes. In this study, eight buffers were created based on the distance to streams, i.e. 0–25, 25–50, 50–75, 75–100, 100–150, 150–200, 200–250, and >250 m. Most of the historical landslides were located between 0 and 75 m from a stream (Table 1).

3.10 Drainage Density

Drainage density is the proportion of the total length of the water flow to the total area of the drainage basin. It is a measure of how well a watershed is drained by river channels. A high drainage density indicates a low infiltration capacity and a quick surface runoff (Nagarajan et al. 2000; Cevik and Topal 2003; Nandi and Shakoor 2009). Drainage networks in this study were extracted directly from the DEM. Eight drainage buffer zones were produced to define the extent of slope instability caused by streams. These drainage buffer zones were: Zone A ($0-0.0025\text{ m}^{-1}$), Zone B ($0.0025-0.005\text{ m}^{-1}$), Zone C ($0.005-0.0075\text{ m}^{-1}$), Zone D ($0.0075-0.01\text{ m}^{-1}$), Zone E ($0.01-0.0125\text{ m}^{-1}$), Zone F ($0.0125-0.015\text{ m}^{-1}$), Zone G ($0.015-0.03\text{ m}^{-1}$), and Zone H ($0.03-0.135\text{ m}^{-1}$). The drainage density analyses showed that all the historical landslides occurred within the density range of $0-0.015\text{ m}^{-1}$ (Table 1).

Table 2 Consistency index of random matrix

<i>N</i>	1	2	3	4	5	6	7	8	9	10
Consistency index of random matrix, <i>IR</i>	0	0	0.58	0.9	1.12	1.24	1.32	1.41	1.45	1.49

* *N* in symmetric matrix ($n \times m$) equal to the number of columns

3.11 Topographic Wetness Index (TWI)

The TWI is a ratio of contributing catchment area to slope inclination (Wilson and Gallant 2000). TWI values estimate soil moisture, or the degree of surface saturation and subsurface soils on land gradients that are correlated to slope instability. TWI is calculated as: $\text{Ln} [A_S/\text{TAN}(\beta)]$, where A_S is the specific catchment area of each cell and β represents the slope gradient (in degrees) of the topographic heights (Moore et al. 1988). The study area was divided into eight different classes of TWI ranging from 0 to 19.3. Table 1 shows that 35.76 % of the historical landslides occurred within the TWI range of 11.04–17.9.

3.12 Stream Power Index (SPI)

The SPI is a way of measuring the power of surface water to erode surfaces based on the hypotheses that discharge (q) is proportional to the specific catchment area (A_S). The SPI value is governed by two parameters: viscosity of the land slope and steepness of the terrain. The SPI is expressed as $\text{SPI} = \text{Ln} [A_S * \text{TAN}(\beta)]$ (Moore et al. 1988). Seven SPI classes were used in this study and they ranged from 0 to 16.6. The SPI analysis showed that 57 % of the historical landslides occurred within the SPI range of 10.44–15.56 (Table 1).

4 Analysis of Landslide Susceptibility

In this study, analyses of the susceptibility to landslides was carried out using the AHP and probabilistic frequency ratio models. Prior to the analyses, the factors affecting landslides in Hulu Kelang area were identified. Landslide regions were defined using the landslide inventory map and satellite images.

4.1 Analytical Hierarchy Process (AHP)

One method of analyzing complex decisions based on quantifiable and tangible criteria is the AHP (Vargas

1990). AHP breaks an unstructured and complex problem down into simple component parameters and then arranges them in hierarchic order, gives them a numerical value that reflects their relative importance before finally defining the priorities to be assigned to the parameters (Saaty and Vargas 2001). This technique has been used successfully to map landslide susceptibility (Ayalew et al. 2004, 2005; Komac 2006; Yoshimatsu and Abe 2006; Akgün et al. 2007, 2008; Castellanos EA and Van-Westen CJ 2007).

AHP involves structuring a problem into primary and secondary objectives. Upon establishment of the hierarchy, a pairwise comparison matrix for each factor in each level is constructed. Each factor is weighed against other factors within the same level, and correlate to the levels above and below its position. The entire scheme is mathematically joined, resulting in a priority statement for each individual or group (Table 1).

The consistency of a matrix was checked by calculating the consistency ratio (*CR*):

$$CR = \frac{CI}{RI} \quad (1)$$

where *RI* is the average value of the consistency index (Table 2) created using a random matrix that depends on the matrix order and *CI* is the consistency index (Saaty 1977). A matrix with a satisfactory consistency level should yield a *CR* of <0.10 . The consistency index (*CI*) and average *RI* obtained from the matrices 11×11 in the present study were 0.453 and 1.51, respectively yielding an consistency ratio (*CR*) of 0.03. The low consistency ratio (<0.10) implied that the computed weight for each factor was acceptable.

4.2 Probabilistic Frequency Ratio Model

The probabilistic frequency ratio method is based on the distribution of landslides and the parameters related to landslides so that the correlation between the location of the landslide and the parameters for the area can be represented (Pradhan et al. 2010). The first

step was to calculate the frequency ratio for each parameter based on its relationship to landslides, as shown in Table 1. Next, the frequency ratio for the sub-criteria of each parameter was calculated. These ratios were used to find the landslide susceptibility index (LSI; refer to Eq. 1; Lee and Pradhan 2007).

$$LSI = Fr_1 + Fr_2 + Fr_3 + \dots + Fr_n \quad (2)$$

where, Fr is the rating for each parameter. According to the probabilistic frequency ratio method, an average LSI has a value of unity. A value of >1 indicates that there is a strong relationship between the landslide and the parameter being investigated (Akgun et al. 2007).

5 Results and Discussion

The landslide susceptibility maps were determined using six different weighting procedures in a GIS-based tool; very low (the lowest susceptibility), low, moderate, high, very high, and critical (The highest class) susceptibility. The area and distribution percentage of the susceptibility landslide classes in the study area were prepared as a conclusion of the two different methods; AHP and probability–FR models.

5.1 Application of Analytical Hierarchy Process Model (AHP)

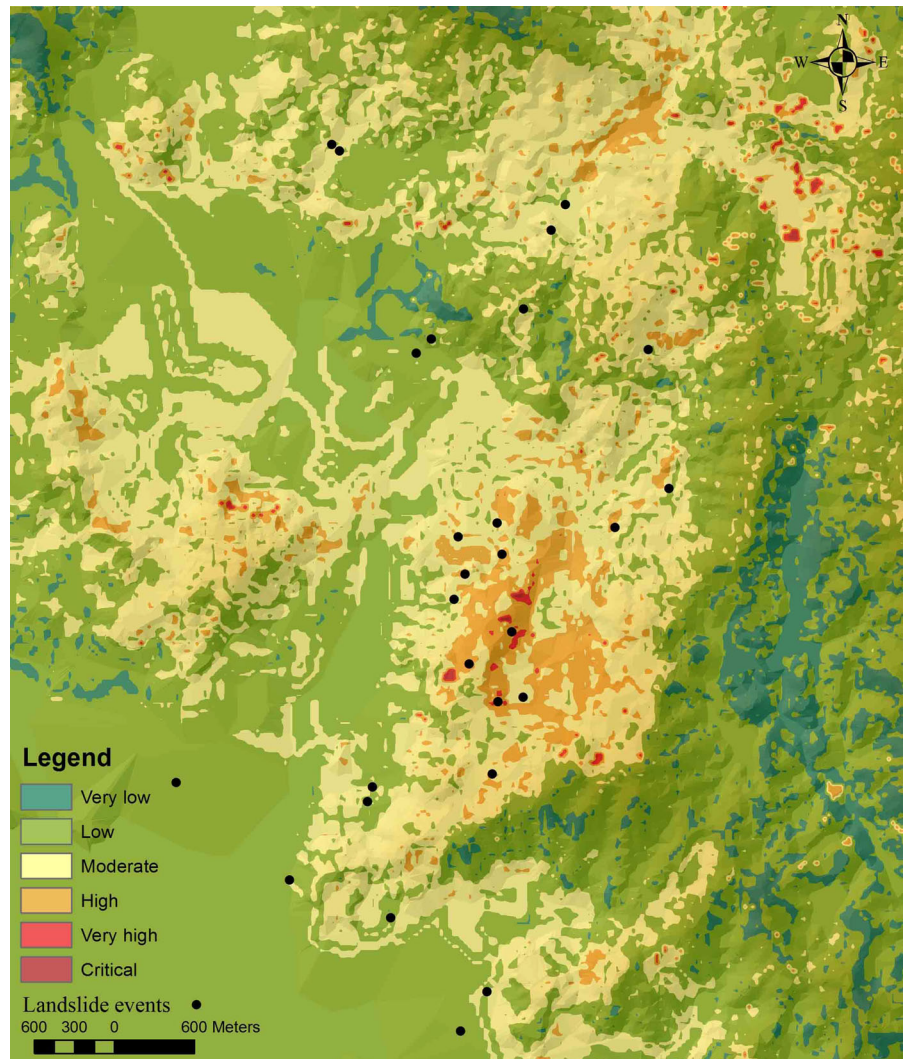
The conclusions of spatial relationship between landslides and landslide conditioning factors using AHP model is shown in Table 1. The geological characteristic of the study area is consisting of three classes of lithological units; granitic rocks, phyllite-schist, and limestone with minor intercalations of phyllite. The AHP was higher (0.571) in granite and (0.286) phyllite-schist and lower (0.143) in limestone bedrocks. Investigation of soil type showed that granite residual soil and phyllite residual soil are more suitable for landslide occurrence with AHP model. In the case of land cover, higher frequency ratio value was seen for grassland (0.315) and rubber region (0.285) types of land cover. This result referred to anthropogenic (human-caused) interpositions such as land cover change. The slope inclination classes showed that 50–90° classes have higher FR weight (0.296). As the slope inclination increases, the shear strength in the soil or other unconsolidated soil layers generally decreases. In the case of slope aspect, most

of the slope failures occurred in north-east and south-west facing. This condition may be conclusion of direction of the two monsoon influenced in this area. The plan curvature values expose the morphology of the terrain surface. A positive curvature is an upwardly convex cell, and a negative curvature is upwardly concave cell. Concave regions have a higher AHP value (0.588) than convex lands. The curvature area, in turn, will increase the moisture content, which will remain saturated, increase erosion and decrease slope stability. In the case of altitude, both 0–100 and 100–200 m classes have 46.7 and 27.7 % of landslide probability and AHP values of 0.467 and 0.277 respectively. The Hulu Kelang area represents that the elevation ranges from 0 to 425 m above mean sea level and 100 % of landslide located in range of 0–200 m. Road construction activities such as soil excavation, imposing of surcharge load, cut slope, embankment alongside road, and removal of vegetation cover may cause failures to the slopes which are otherwise stable. The distance to roads analyses showed that landslides usually occurred at the distances between 0–25 and 25–50 m respectively (Table 1). The connection between distance to rivers and slope failures indicates direct values. And the distance from rivers augments the constituting of landslide is decreases. The AHP in range between 0–25 and 25–50 m distance show the highest weight (Table 1). In the case of drainage density, the AHP results showed that increasing drainage density has obvious trend in increasing landslide in class 0–0.015 m⁻¹. Relation between TWI and landslide probability showed that 12.76–14.48 class has the highest value of AHP (0.409). Similarly, for SPI, class 10.44–12.55 has the most AHP value (0.275). On conclusion of the analyses the frequency of each layer's classes was defined, and a LSI map (Fig. 3) was yielded by the landslide susceptibility map using AHP model.

5.2 Application of Frequency Ratio Model

Similarly, the conclusions of spatial relationship between landslides and landslide conditioning factors using FR model is represented in Table 1. In the case of the lithology, Granite rock includes 1.345 of the higher FR with 74 % of landslide events. The land cover factor is very important for landslide susceptibility studies, particularly the mostly of hazard regions

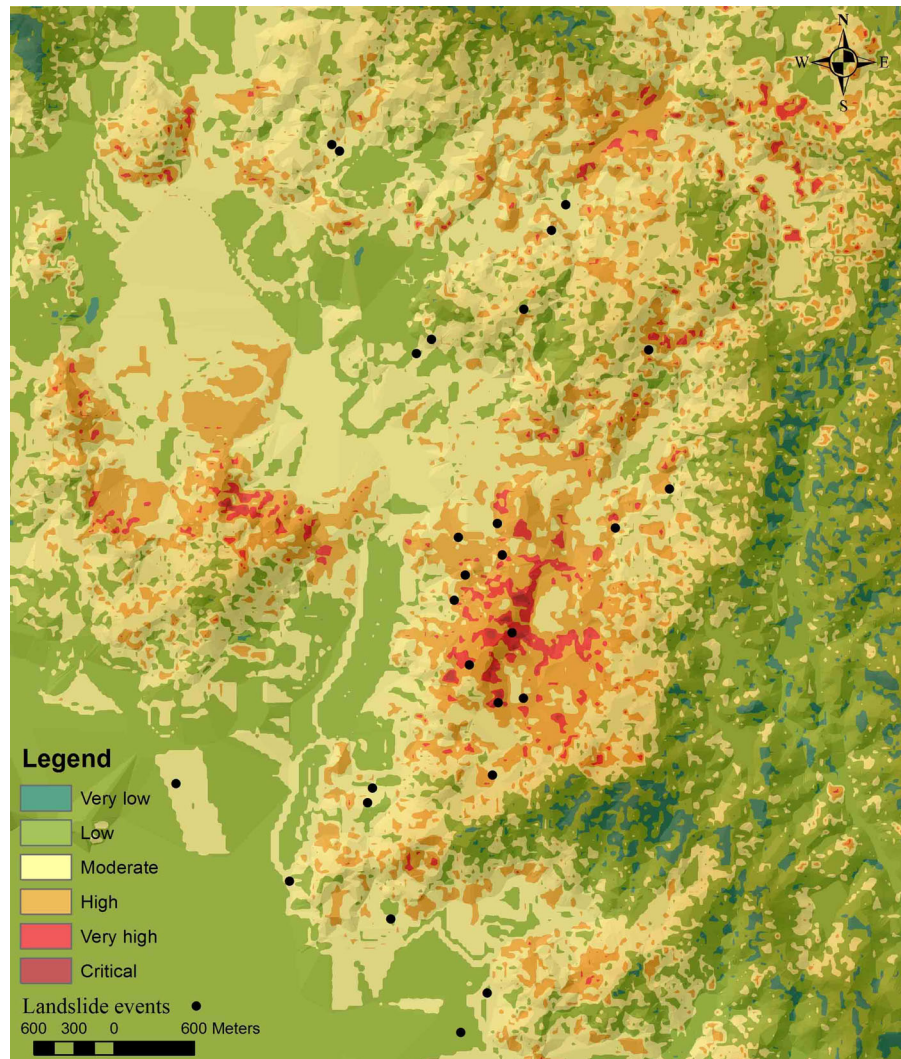
Fig. 3 Landslide susceptibility map produced from AHP model



that are covered with different vegetation. Rubber plantation, grassland, and secondary jungle lands display more saturation and greater landslides than other places. Slope failures are largely represented in rubber and grassland areas. The rubber and grass areas are the result of land cover change, Progressive forest clearing, and conversion to rubber plantation. The potential of the landslide events is high in these regions, the FR being 2.50 and 2.11, respectively (Table 1). The connection between slope failures and slope inclination gives direct values. Normally, the increase of slope degree propagates the landslide constituting should be growth. Accordingly, in this study, the increase of slope degree develops the landslide constituting rises (Table 1). 100 % of

landslide events located in slope range of 0° – 50° include 0° – 10° (0.941), 10° – 20° (1.679), 20° – 30° (0.743), 30° – 40° (0.656), and 40° – 50° (2.474) of the higher FR, respectively. In the case of slope aspect, the estimation of the slope aspect parameter on North-facing slopes represents high probability (1.891) of landslide occurrence (Table 1). In the case of plan curvature, Concave lands have a higher FR value (0.588) than convex lands. The elevation–landslide analysis determined that landslides frequently occurred from sea level to 200 m; in specific, the FR is very high in the elevation range of 100–200 m (Table 1). Conclusions defined that the FR values decreased with the altitude growth in the study area (Table 1). In the case of distance from roads, higher

Fig. 4 Landslide susceptibility map produced from probability-frequency ratio (FR) model



FR value 0.650, 0.907 were found for distances between 0–25 and 25–50 m respectively. In the study area, road construction and embankment erosion are the most important factors in land gradient imbalance causing frequent occurrence of slope failures. Assessment of distance from rivers is represented that distance of 0–75 m have high correlation with landslide occurrence (Table 1). From this observation, we can conclude that the general trend of the FR value decreases with the distance from the rivers and roads. In the case of drainage density, most of the landslides occurred in 0–0.0025 m^{-1} class (FR value of 0.439). The relation between TWI and landslide probability indicated that class between 12.76–14.48 has most FR value. Similarly, for SPI values, 10.44 and 12.15 class

has the highest value of FR 1.968. On conclusion of the analysis the frequency of each layer's classes was defined, and a LSI map (Fig. 4) was yielded by the landslide susceptibility map using FR model.

5.3 Validation of the Susceptibility Maps

5.3.1 Receiver Operating Characteristics (ROC)

The final landslide susceptibility maps were evaluated in regards to unknown future landslides (Chung and Fabbri 2003). A ROC curve is an effective way to indicate the quality of probabilistic and deterministic findings and forecast systems (Swets 1988). In this study a ROC curve test was used as a cross-validation

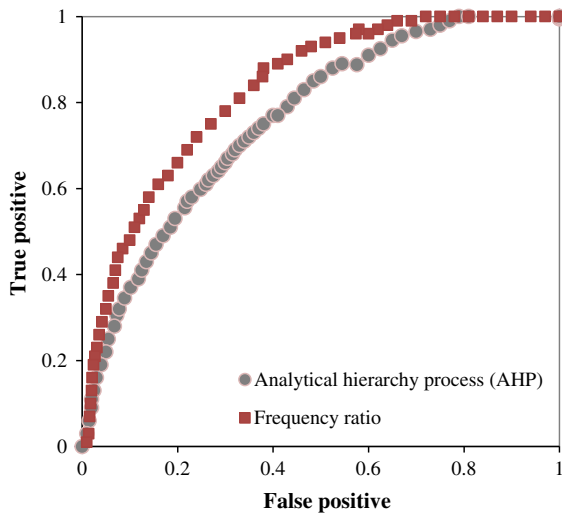


Fig. 5 Success rate curves for the two landslide susceptibility maps

method. First, the historical landslide events were divided into two groups. The modeling group, which represented approximately 70 % of the total landslides, was used as a training set to construct the susceptibility maps. The remaining 30 % of landslides were used for prediction testing. The regions that were not affected by landslides were used as prediction group during the training phase. The regions affected by landslides were used in the training set labeled “areas prone to landslides”. The true positive rate of the Y-axis and the false positive rate of the X-axis were plotted using the ROC curve. This value ranged from 0.5, which indicated a random prediction, represented by the diagonal straight line, to one, which indicated an excellent prediction that could be used to collect the relative ranks for each prediction type (Cervi et al. 2010). In this study, the percentage of unstable pixels was correctly predicted by the model as was the specificity validation or the percentage of predicted unstable pixels. The result of sensitivity analysis indicated that the probabilistic FR model (Fig. 5) was more efficient in terms of its predictions when compared to AHP model used in this study. The area under curve (AUC) for the landslide susceptibility map produced using the probabilistic frequency ratio model was 0.8154 (prediction accuracy = 81.5 %) as determined by the ROC plot assessment. The AUC for the AHP model has shown 0.7130 (Table 3). With respect to predicted unstable pixels (Fig. 6), the AUC for the probabilistic frequency ratio was also the highest

Table 3 Comparison of success rate curves for the four landslide susceptibility maps

Model	AUC	Prediction
Probability–frequency ratio	0.8154	Very good
Analytical hierarchy process (AHP)	0.7130	good

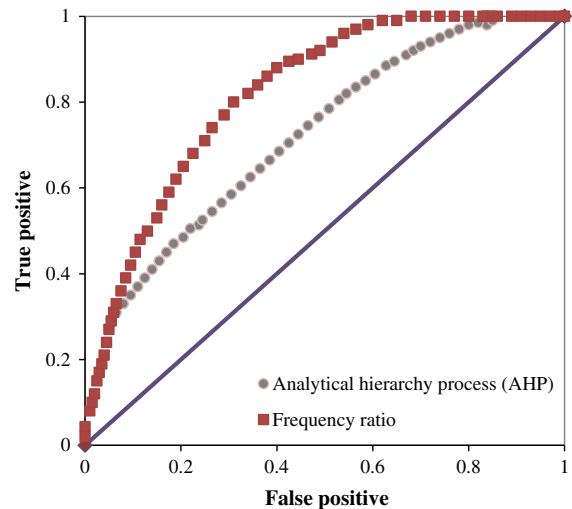


Fig. 6 Prediction rate curves for the two landslide susceptibility maps

Table 4 Comparison of prediction rate curves for the four landslide susceptibility maps

Model	AUC	Prediction
Probability–frequency ratio	0.7904	good
Analytical hierarchy process (AHP)	0.6787	moderate

(0.7904), and the AHP model was lower than FR by 0.6787 (Table 4). From the ROC curve test, it can be concluded that the probabilistic frequency ratio model was the best modeling technique used in this study.

6 Prediction of Landslides

One main objective of this study was to evaluate the spatial predictability of landslide events in Hulu Kelang area, using the AHP and probability-FR

models for regional landslide hazard assessment. The success of landslide prediction model has been typically evaluated by comparing locations of measured landslides with the predicted results. Thus, the landslide ratio of each predicted hazard class (landslide ratio for each predicted hazard class) was employed for evaluating the performance of the landslide model. Landslide ratio for each predicted hazard class (LRclass) was based on the ratio of landslide sites contained in each hazard class, in relation to the total number of actual landslide sites, according to the predicted percentage of area in each class of hazard category.

$$LR_{class} = \frac{\% \text{ of contained landslide sites in each class of hazard}}{\% \text{ of predicted landslide areas in each class of hazard}}$$

Note that in the numerator, the number of landslide sites, instead of the number of landslide cells, is used. The performance value derived by LRclass enables consideration of predicted stable areas as well as predicted unstable areas, and thus substantially reduces the over-prediction of landslide potential. Unlike the numerator, the number of predicted and total cells is used in denominator. The numerator, also, is the same as the SR (success ratio) index. Tables 5 and 6 show that 5.1 and 15.09 % of the area were classified as unstable (hazardous area ≥ high), and

that 33 and 49 % of the actual landslides were correctly localized within this predicted unstable areas, respectively. AHP model represented the $LR_{FS} \geq \text{high}$ about 17.2 by calculating the % of LRclass equal to 90.27 %. The % of $LR_{FS} \geq \text{high}$ of FR model presented about 96.37 % by calculating the LRclass equal to 35.17, if a landslide happens, then predicted unstable area (hazardous area ≥ high) has 90 % chance of including the landslide.

7 Conclusion

This paper provides a susceptibility assessment of shallow landslides in Hulu Kelang area, Kuala Lumpur, Malaysia using AHP and probability–FR methods. Two landslide susceptibility maps were produced and their reliabilities were verified by the ROC and active landslide zones. The susceptibility level was classified into five categories, namely equal, moderate, high, very high, and extreme. The spatial distributions of the landslide susceptibility zones showed that most of the landslide prone areas located near the toe of hillsides with intensive new developments. The relatively flat and well developed areas at the east of Hulu Kelang are less susceptible to landslide. The prediction rate of ROC curves for the susceptibility maps

Table 5 Summary of AHP model results in landslide simulations

AHP	Landslide site (a)	% of landslide site (c) = a/b	% of predicted area (d)	LRclass (e) = c/d	% of LRclass = e/f
Very low	4	2	7.30	0.22	1.16
Low	82	33	56.83	0.58	3.05
Moderate	80	32	30.77	1.05	5.50
High	75	30	4.67	6.47	33.96
Very high	8	3	0.30	10.73	56.31
Critical	0	0	0.13	0	0
Sum	249 (b)	100.000	100.00	19.06 (f)	100.00

Table 6 Summary of FR model results in landslide simulations

FR	Landslide site (a)	% of landslide site (c) = a/b	% of predicted area (d)	LRclass (e) = c/d	% of LRclass = e/f
Very low	0	0	4.34	0.00	0.00
Low	28	11	43.22	0.26	0.72
Moderate	99	40	37.35	1.07	2.93
High	83	33	12.89	2.60	7.11
Very high	27	11	2.02	5.38	14.75
Critical	12	5	0.18	27.19	74.51
Sum	202 (b)	100.000	100.00	36.49(f)	100.00

indicated that the probabilistic frequency ratio model had the highest prediction accuracy (>81 %), while the AHP model showed the middle prediction accuracy (71.3 %). A landslide susceptibility map for Hulu Kelang area was successfully developed. And the field observation verification results showed that 96.37 % of the historical landslide events occurred in the zones of high–very high landslide susceptibility based on FR model. The results proved that the developed landslide susceptibility map is reliable and capable of providing good predictions on the spatial distributions of landslide occurrence in the study area.

Acknowledgments The authors acknowledge and appreciate the provisions of rainfall and landslide data by the Ampang Jaya Municipal Council (MPAJ), the Slope Engineering Branch of Public Works Department Malaysia (PWD), and the Department of Irrigation and Drainage Malaysia (DID), without which this study would not have been possible.

References

- Akgün A, Bulut F (2007) GIS-based landslide susceptibility for Arsin-Yomra (Trabzon, North Turkey) region. *Environ Geol* 51:1348–1377
- Akgün A, Dag S, Bulut F (2008) Landslide susceptibility mapping for landslide-prone area (Findikli, NE Turkey) by likelihood frequency ratio and weighted linear combination models. *Environ Geol* 54:1127–1143
- Ali F (2000) Unsaturated tropical residual soils and rainfall induced slopes in Malaysia. *Asian Conference on Unsaturated Soils Singapore* 41(52):18–19
- Ayalew L, Yamagishi H (2005) The application of GIS-based logistic regression for landslide susceptibility mapping in the Kakuda-Yahiko mountains. *Cent Jpn Geomorphol* 65:15–31
- Ayalew L, Yamagishi H, Ugawa N (2004) Landslide susceptibility mapping using GIS-based weighted linear combination, the case in Tsugawa area of Agano River, Niigata prefecture. *Jpn Landslides* 1:73–81
- Ayalew L, Yamagishi H, Marui H, Kanno T (2005) Landslides in Sado Island of Japan: part II. GIS-based susceptibility mapping with comparisons of results from two methods and verifications. *Eng Geol* 81:432–445
- Castellanos Abella EA, Van Westen CJ (2007) Generation of landslide risk index map for Cuba using spatial multi-criteria evaluation. *Landslides* 4:311–325
- Cervi F, Berti M, Borgatti L, Ronchetti F, Manenti F, Corsini A (2010) Comparing predictive capability of statistical and deterministic methods for landslide susceptibility mapping: a case study in the northern Apennines (Reggio Emilia Province, Italy). *Landslides* 7:433–444
- Cevik E, Topal T (2003) GIS-based landslide susceptibility mapping for a problematic segment of the natural gas pipeline, Hendek (Turkey). *Environ Geol* 44:949–962
- Chigira M, Nakamoto M, Nakata E (2002) Weathering mechanisms and their effects on the landsliding of ignimbrite subject to vapor-phase crystallization in the Shirakawa pyroclastic flow, northern Japan. *Eng Geol* 66(1–2):111–125
- Chung CJF, Fabbri AG (2003) Validation of spatial prediction models for landslide hazard mapping. *Nat Hazards* 30:451–472
- Dai FC, Lee CF, Li J, Xu ZW (2001) Assessment of landslide susceptibility on the natural terrain of Lantau Island. *Hong Kong. Environ Geol* 43(3):381–391
- Dai FC, Lee CF, Ngai YY (2002) Landslide risk assessment and management: an overview. *Eng Geol* 64(1):65–87
- D'Amato Avanzi G, Giannecchini R, Puccinelli A (2004) The influence of the geological and geomorphological settings on shallow landslides. An example in a temperate climate environment: the June 19, 1996 event in northwestern Tuscany (Italy). *Eng Geol* 73:215–228
- Derbyshire E, Wang J, Meng X (2000) A treacherous terrain: background to natural hazards in northern China with special reference to the history of landslide in Gansu Province, in *Landslides in the Thick Loess Terrain of North-West China*. Wiley, Chichester, UK, pp 1–19
- Ercanoglu M (2005) Landslide susceptibility assessment of SE Bartın (West Black Sea region, Turkey) by artificial neural networks. *Nat Hazards Earth Syst Sci* 5:979–992
- Ercanoglu M, Gokceoglu C, Van Asch THWJ (2004) Landslide susceptibility zoning north of Yenice (NW Turkey) by multivariate statistical techniques. *Nat Hazards* 32:1–23
- Ercanoglu M, Kasmer O, Temiz N (2008) Adaptation and comparison of expert opinion to analytical hierarchy process for landslide susceptibility mapping. *Bull. Eng Geol Environ* 67:565–578
- Farisham AS (2007) Landslides in the hillside development in the Hulu Klang, Klang Valley. *Post-Graduate Seminar, UTM, Skudai, Malaysia*
- Guzzetti F, Carrara A, Cardinali M, Reichenbach P (2006) Landslide hazard evaluation: a review of current techniques and their application in a multi-scale study. *Cent Italy. Geomorphology* 31:181–216
- Komac M (2006) A landslide susceptibility model using the analytical hierarchy process method and multivariate statistics in perialpine Slovenia. *Geomorphology* 74(1–4): 17–28
- Lee S (2005) Application of logistic regression model and its validation for landslide susceptibility mapping using GIS and remote sensing data. *Int J Remote Sens* 26:1477–1491
- Lee S, Pradhan B (2007) Landslide hazard mapping at Selangor, Malaysia using frequency ratio and logistic regression models. *Landslides* 4:33–41
- Lee S, Choi J, Min K (2004a) Probabilistic landslide hazard mapping using GIS and remote sensing data at Boun. Korea. *Int J Remote Sens* 25(11):2037–2052
- Lee S, Ryu J, Won J, Park H (2004b) Determination and application of the weight for landslide susceptibility mapping using an artificial neural network. *Eng Geol* 71:289–302
- Low TH, Ali F (2012) Slope hazard assessment in urbanized area. *Electron J Geotech Eng* 17(C):341–352

- Moore ID, O'Loughlin EM, Burch GJ (1988) A contour based topographic model and its hydrologic and ecological applications, *Earth Surf. Process. Landforms* 13: 305–320
- Nagarajan R, Roy A, Vinod Kumar R, Mukherjee A, Khire MV (2000) Landslide hazard susceptibility mapping based on terrain and climatic factors for tropical monsoon regions. *Eng Geol Environ* 58:275–287
- Nandi A, Shakoor A (2009) A GIS-based landslide susceptibility evaluation using bivariate and multivariate statistical analyses. *Eng Geol* 110:11–20
- Nefeslioglu HA, Duman TY, Durmaz S (2008) Landslide susceptibility mapping for a part of tectonic Kelkit Valley (Easten Black Sea Region of Turkey). *Geomorphology* 94:401–418
- Phua MH, Minowa M (2005) Evaluation of environmental functions of tropical forest in Kinabalu Park, Sabah, Malaysia using GIS and remote sensing techniques: implications to forest conservation planning. *J For Res* 5:123–131
- Pradhan B, Lee S (2010) Delineation of landslide hazard areas on Penang Island, Malaysia, by using frequency ratio, logistic regression and artificial neural network models. *Environ Earth Sci* 60:1037–1054
- Saaty TL (1977) A scaling method for priorities in hierarchical structures. *J Math Psychol* 15(3):234–281
- Saaty TL (1980) *The analytic hierarchy process*. McGraw-Hill International, New York
- Saaty TL, Vargas GL (2001) *Models, methods, concepts, and applications of the analytic hierarchy process*. Kluwer Academic Publisher, Boston
- Saha AK, Gupta RP, Arora MK (2002) GIS-based landslide hazard zonation in the Bhagirathi (Ganga) valley, Himalayas. *Int J Remote Sens* 23(2):357–369
- Sidle RC, Chigira M (2004) Landslides and debris flows strike Kyushu, Japan. *Trans Am Geophys Union* 85(15):145–151
- Sidle RC, Ochiai H (2006) Landslides: processes, prediction and land use. *Water Resour Monogr* 18:312
- Sidle RC, Tsuboyama Y, Noguchi S, Hosoda I, Fujieda M, Shimizu T (2000a) Stream flow generation in steep headwaters: a linked hydrogeomorphic paradigm. *Hydrol Process* 14:369–385
- Sidle RC, Kamil I, Sharma A, Yamashita S (2000b) Stream response to subsidence from underground coal mining in central Utah. *Environ Geol* 39(3–4):279–291
- Swets JA (1988) Measuring the accuracy of diagnostic systems. *Science* 240:1285–1293
- Vargas LG (1990) An overview of the analytic hierarchy process and its applications. *Eur J Oper Res* 1(48):2–8
- Wakatsuki T, Tanaka Y, Matsukura Y (2005) Soil slips on weathering-limited slopes underlain by coarse-grained granite or fine-grained gneiss near Seoul, Republic of Korea. *Catena* 60(2):181–203
- Wilson JP, Gallant JC (2000) *Terrain analysis: principles and applications*. Wiley, New York, pp 303
- Yalcin A (2005) An investigation on Ardesen (Rize) region on the basis of landslide susceptibility. Ph.D. dissertation Karadeniz Technical University, Trabzon, Turkey (in Turkish)
- Yalcin A (2008) GIS based landslide susceptibility mapping using analytical hierarchy process and bivariat statistics in Ardesen (Turkey): comparison of results and confirmations. *Catena* 72:1–12
- Yoshimatsu H, Abe S (2006) A review of landslide hazards in Japan and assessment of their susceptibility using analytical hierarchy process (AHP) method. *Landslides* 3:149–158